Supporting Information

Dankers et al. 10.1073/pnas.1302078110

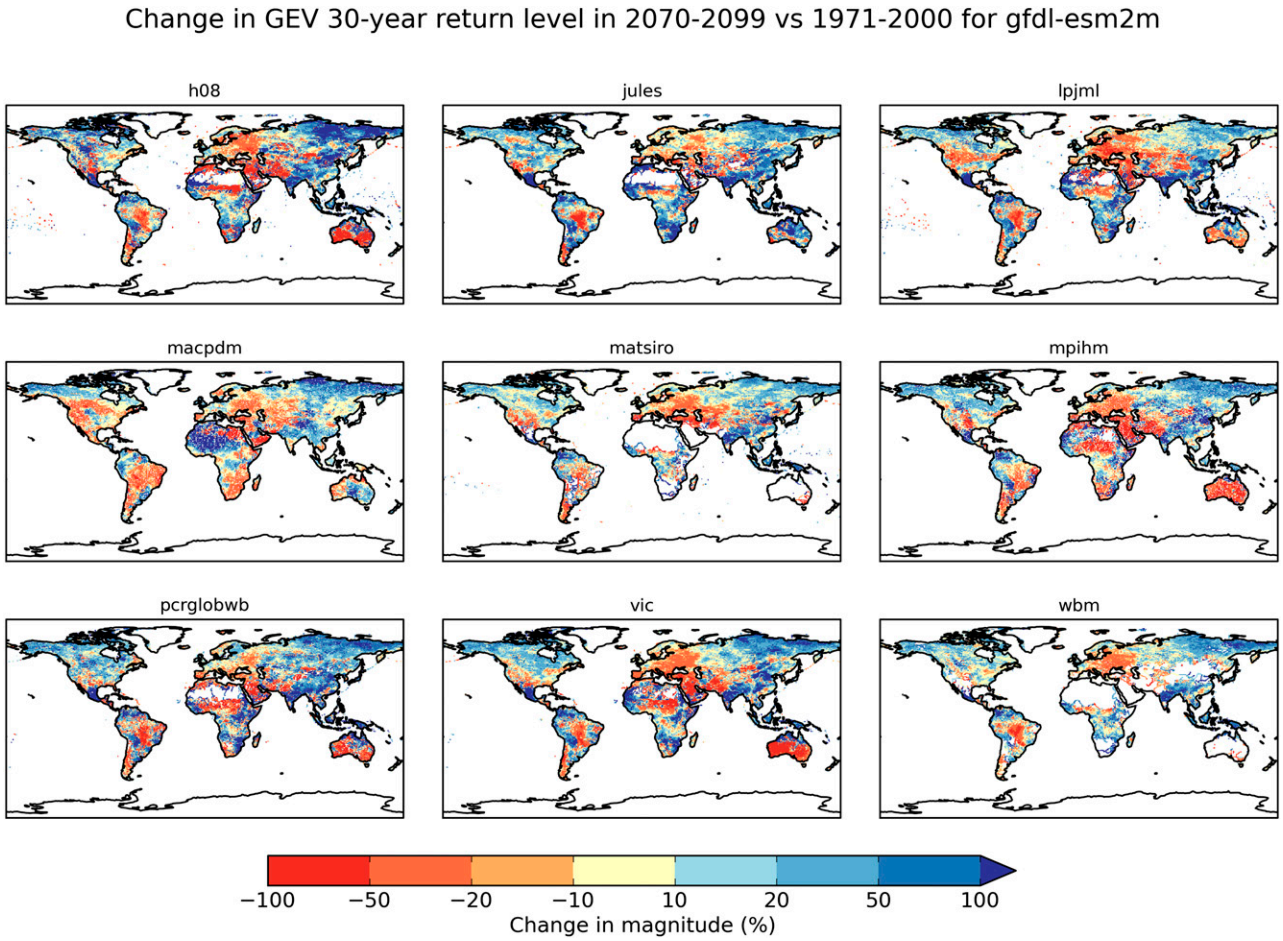

Fig. S1. Change in the magnitude of 30-y return level of river flow (Q30) under future climate conditions (2070–2099; representative concentrations pathway RCP8.5) for GFDL-ESM2M simulations (for full names of the models see Table 1).

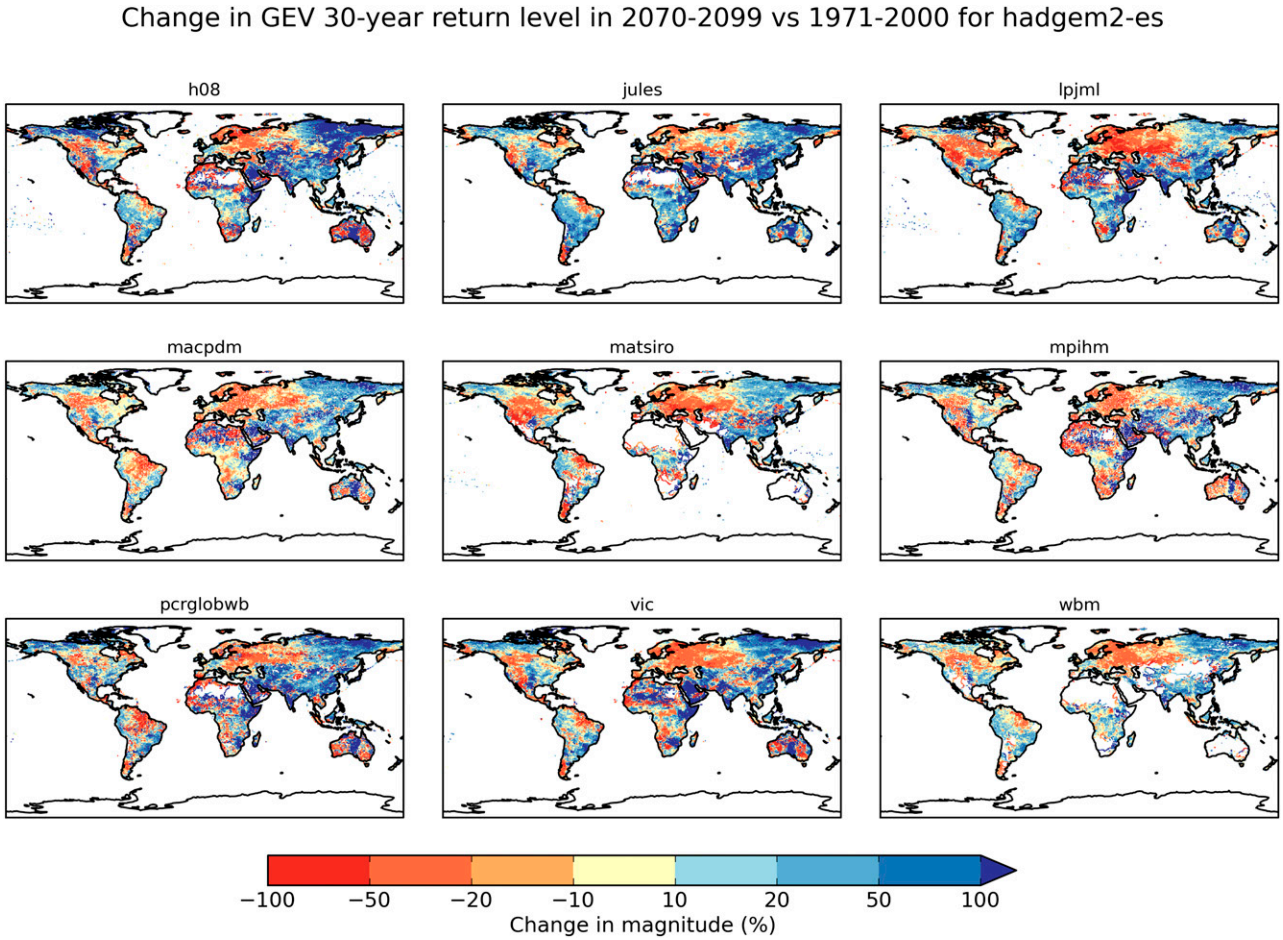

Fig. S2. Change in the magnitude of Q30 under future climate conditions (2070–2099; RCP8.5) for HadGEM2-ES simulations.

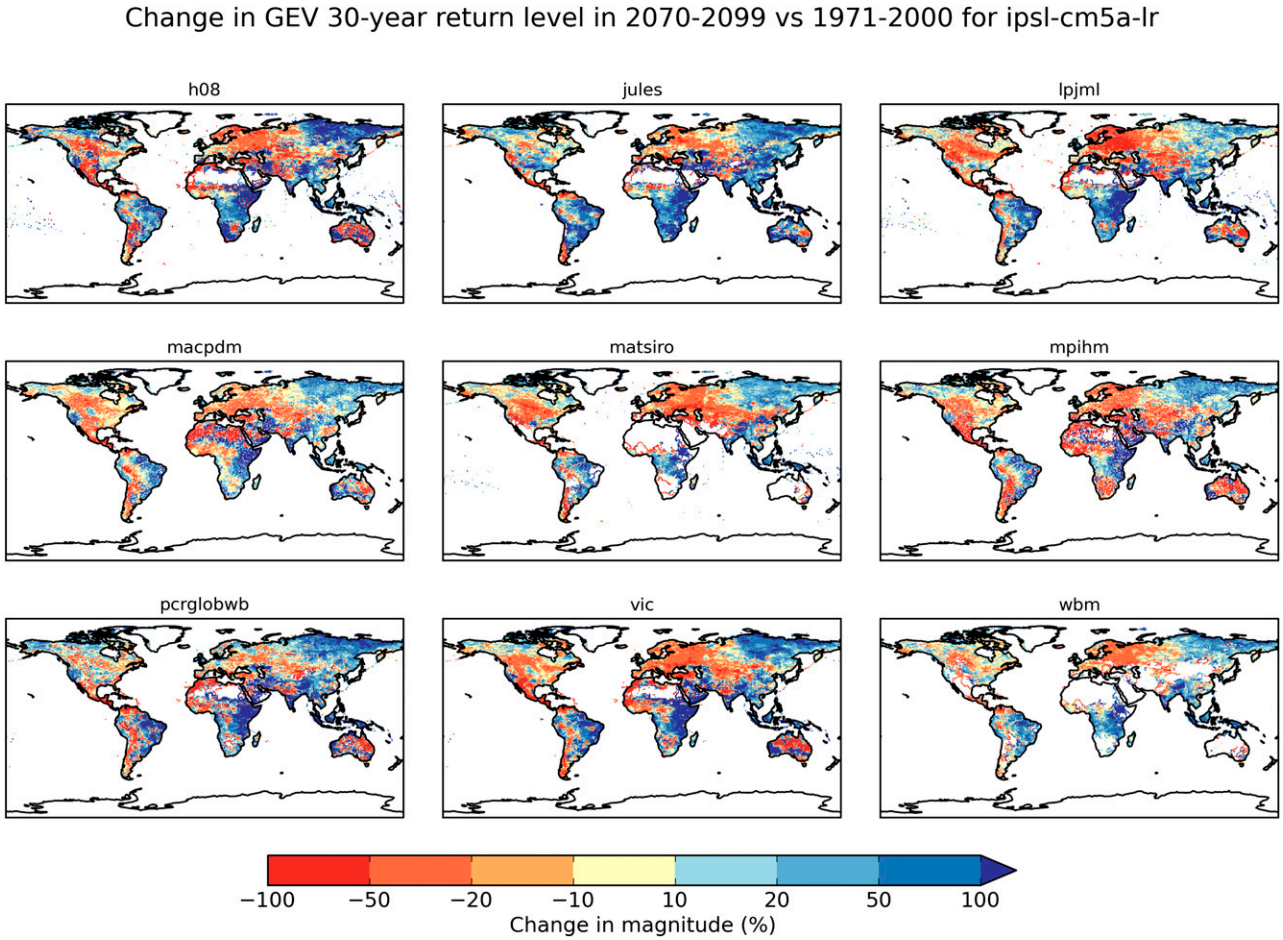

Fig. S3. Change in the magnitude of Q30 under future climate conditions (2070–2099; RCP8.5) for IPSL-CM5A-LR simulations.

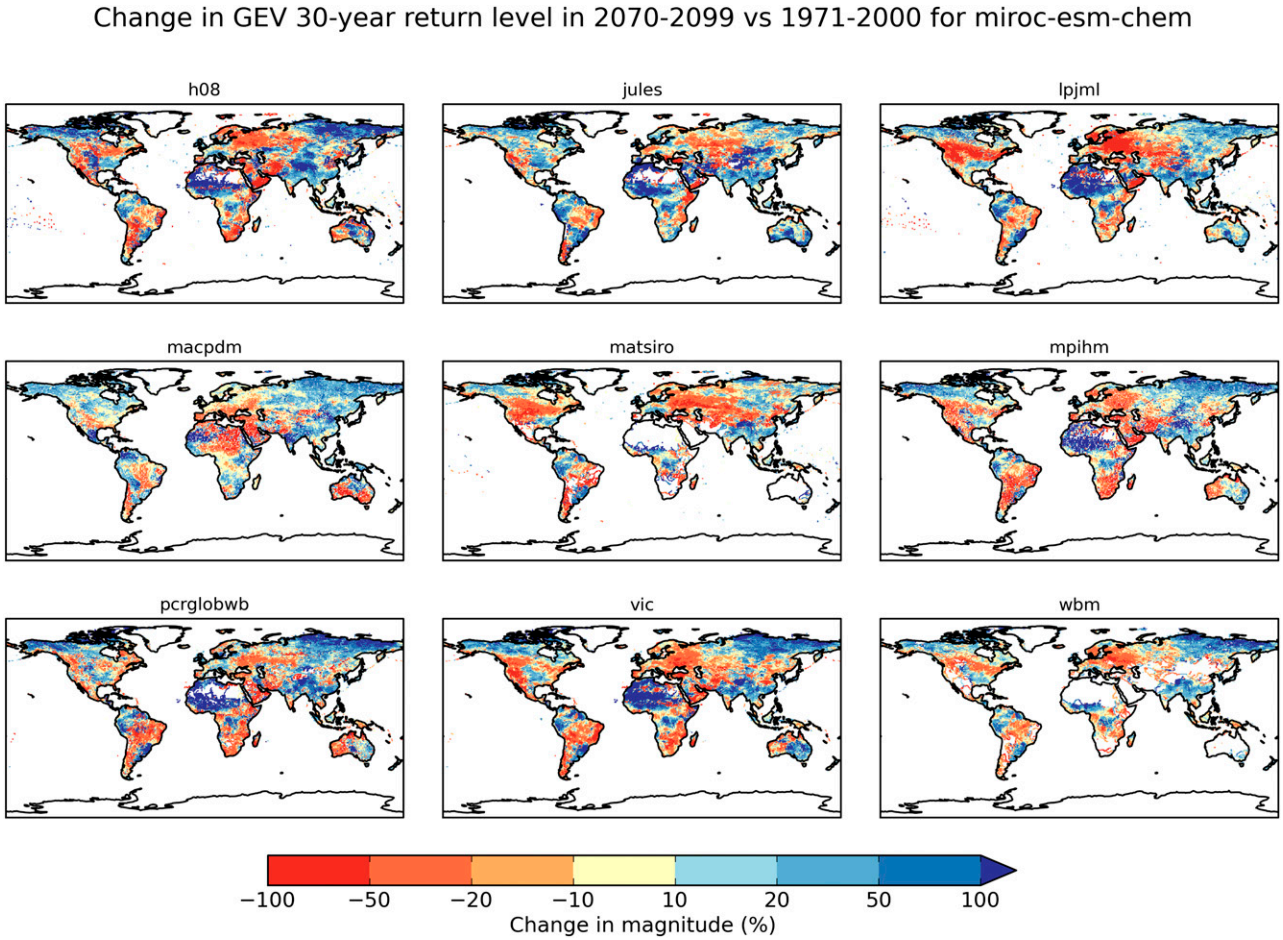

Fig. S4. Change in the magnitude of Q30 under future climate conditions (2070–2099; RCP8.5) for MIROC-ESM-CHEM simulations.

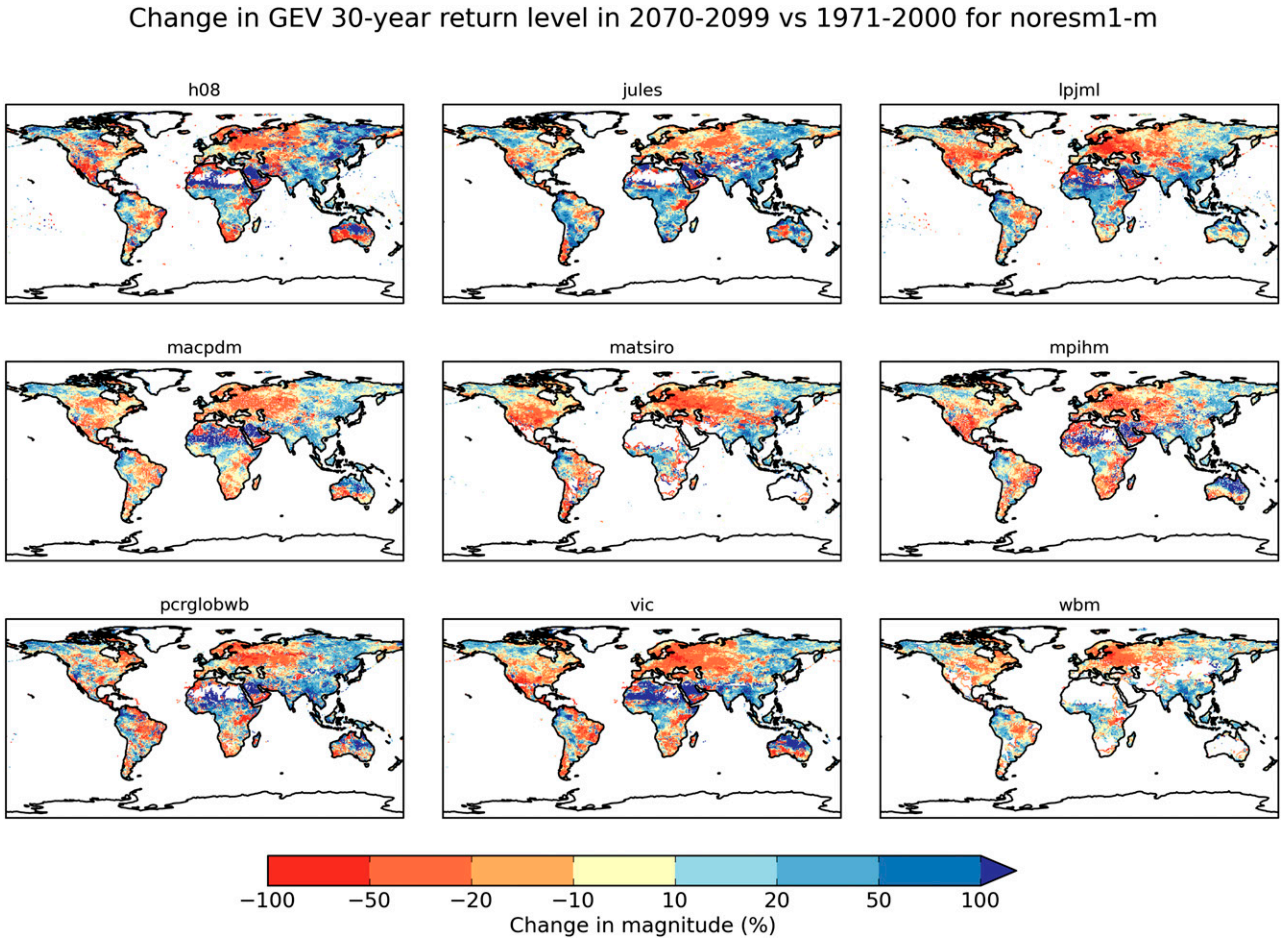

Fig. S5. Change in the magnitude of Q30 under future climate conditions (2070–2099; RCP8.5) for NorESM1-M simulations.

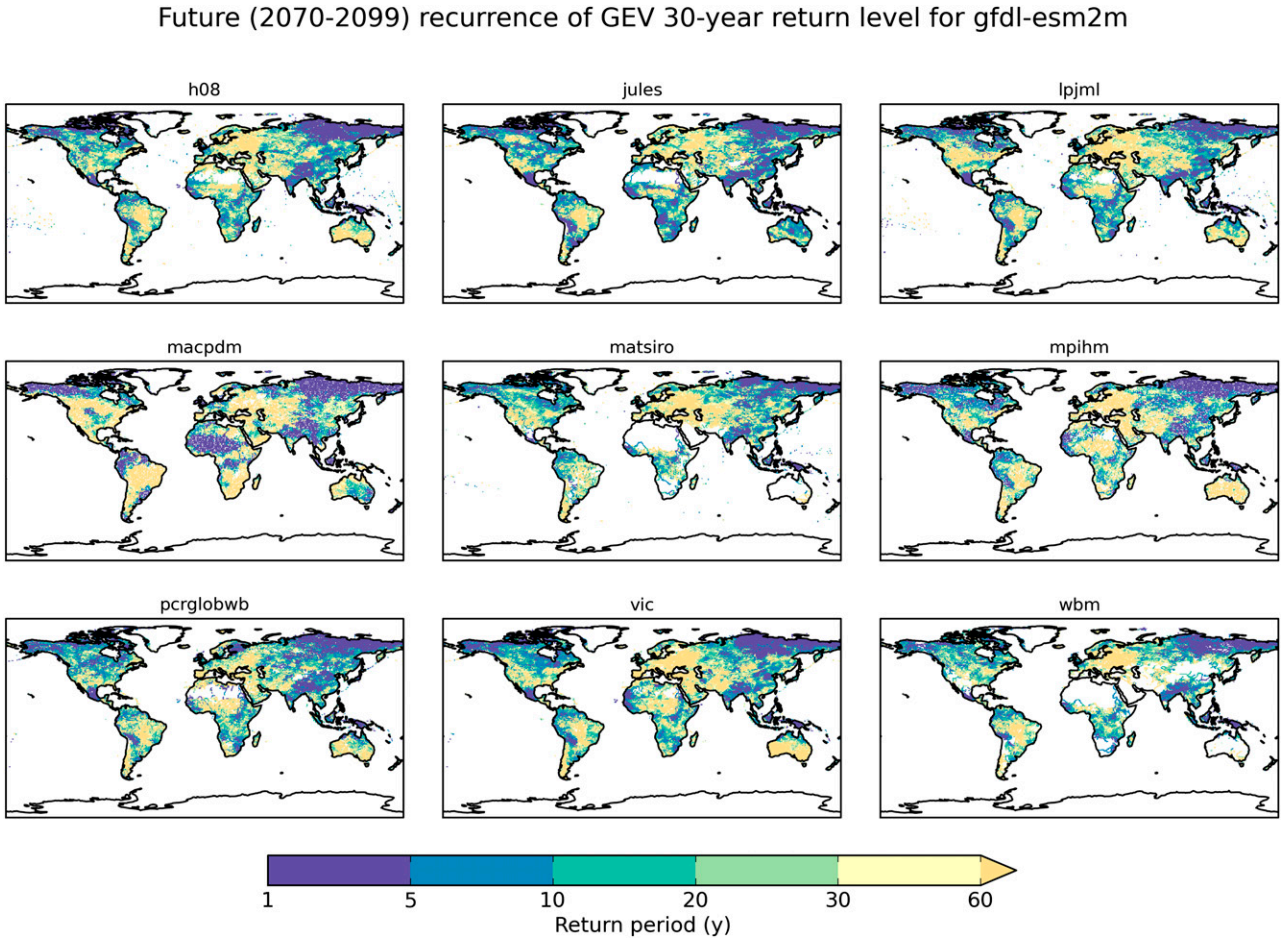

Fig. S6. Estimated future (2070–2099) return period of the historical (1971–2000) Q30 for GFDL-ESM2M simulations.

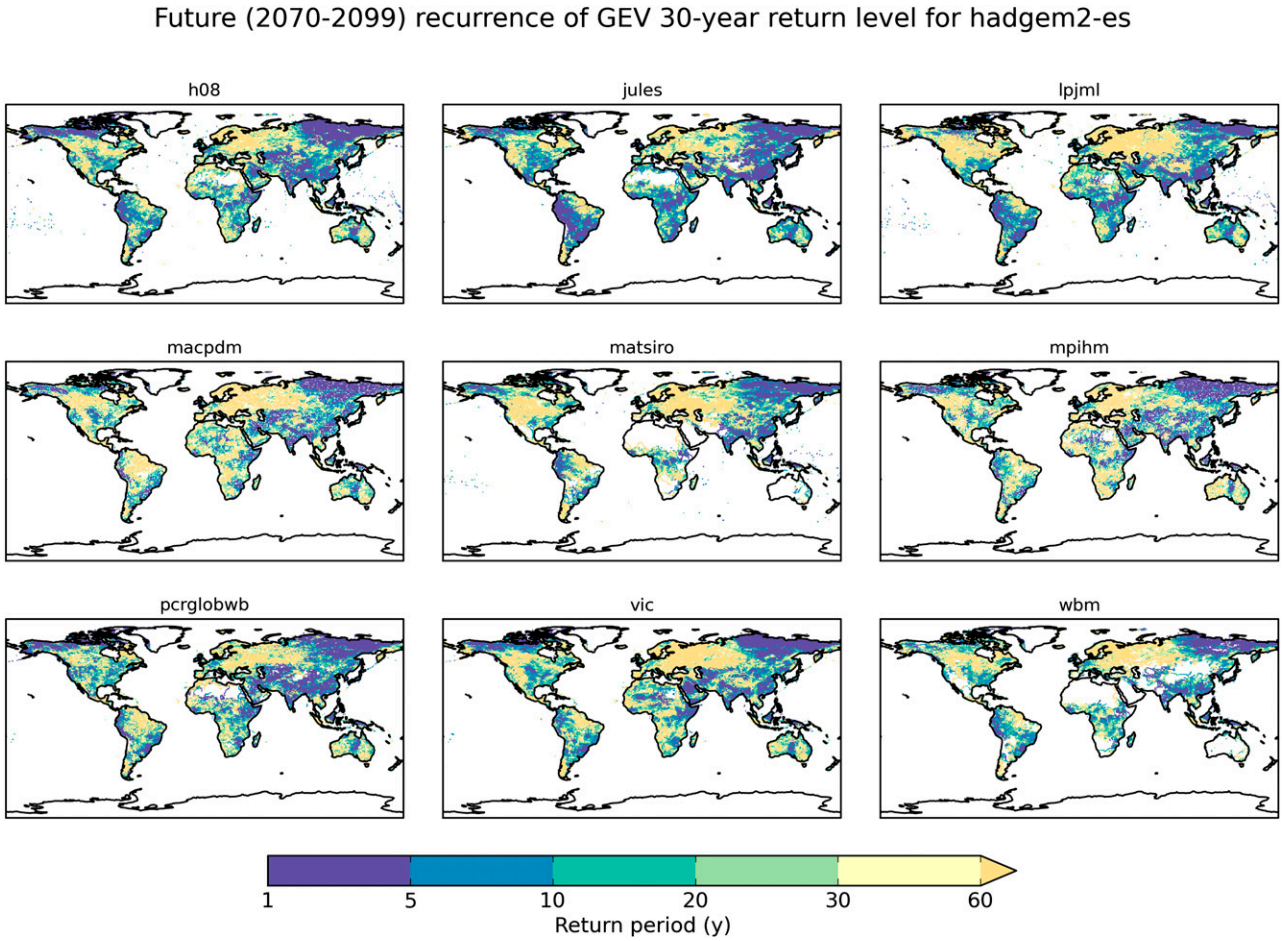

Fig. S7. Estimated future (2070–2099) return period of the historical (1971–2000) Q30 for HadGEM2-ES simulations.

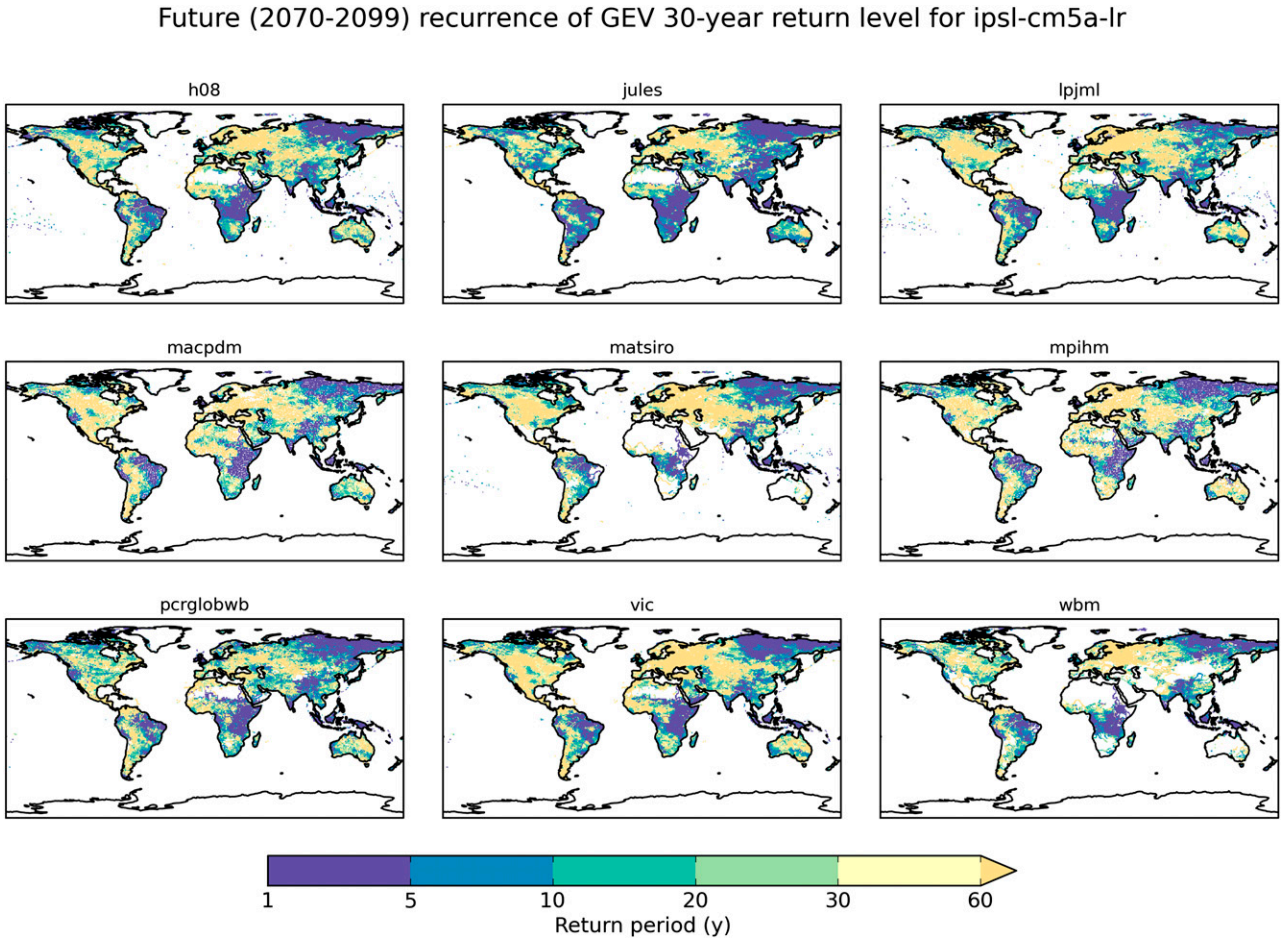

Fig. S8. Estimated future (2070–2099) return period of the historical (1971–2000) Q30 for IPSL-CM5A-LR simulations.

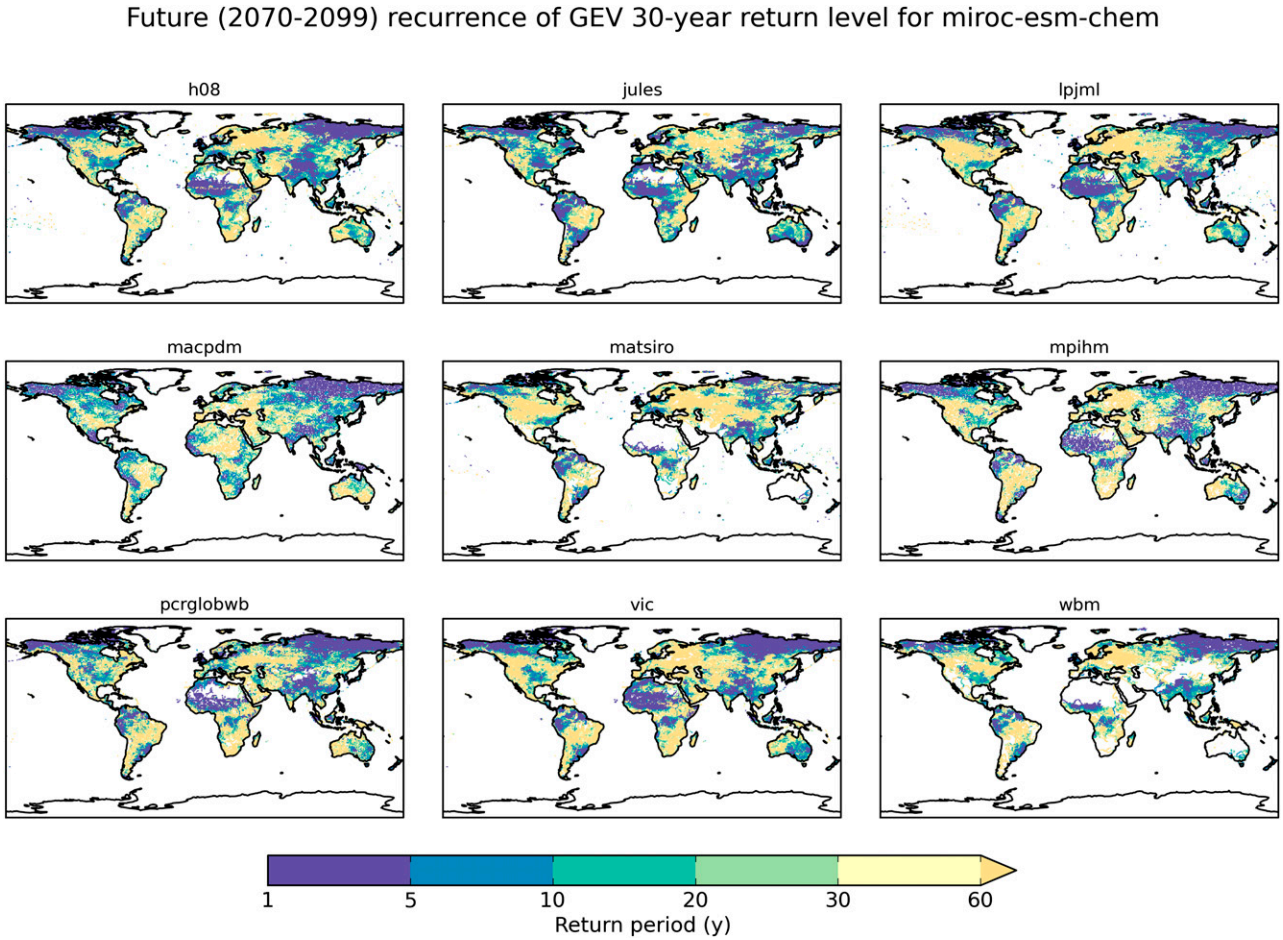

Fig. S9. Estimated future (2070–2099) return period of the historical (1971–2000) Q30 for MIROC-ESM-CHEM simulations.

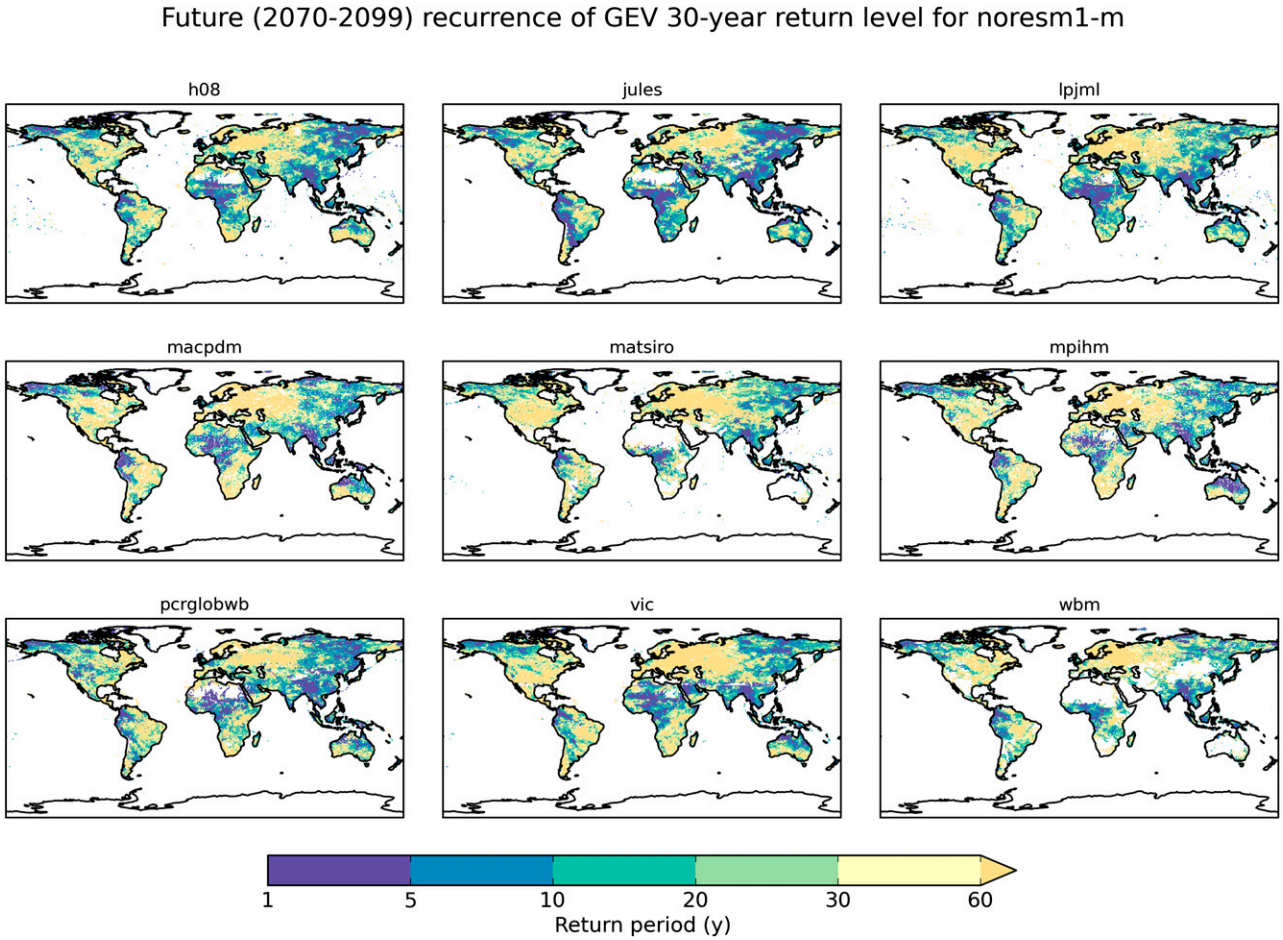

Fig. S10. Estimated future (2070–2099) return period of the historical (1971–2000) Q30 for NorESM1-M simulations.